International Journal of Thermophysics, Vol. 11, No. 5, 1990

Thermodynamic Analysis of Manganese

A. Fernández Guillermet[1] and W. Huang[2]

Received August 23, 1989

A description of the Gibbs energy of the various solid modifications of manganese at 101325 Pa has been obtained for the whole temperature range from 298 K to the melting point. The present analysis accounts for the effect of a magnetic transition in α-, γ-, and δ-Mn, which is treated using the Inden–Hillert–Jarl phenomenological model for the magnetic Gibbs energy. Our description involves smaller magnetic contributions to the entropy of these phases than suggested in the classical work by Weiss and Tauer. An expression for the Gibbs energy of the liquid phase is also reported.

KEY WORDS: enthalpy; Gibbs energy; heat capacity; magnetic entropy; magnetic properties; manganese; transitions.

1. INTRODUCTION

The thermodynamic properties of Mn have been considered on several occasions. Tauer and Weiss [1] presented in 1957 an analysis of the experimental information on α-Mn based on separating the vibrational, electronic and magnetic contributions to the heat capacity. The analysis was extended by Weiss and Tauer [2] to the β, γ, and δ phases in 1958. They reported Gibbs energy differences for all solid phases of Mn.

The thermodynamic information on Mn available in 1967 was compiled by Hultgren et al. [3], who tabulated the properties of each phase in its stable range of temperature from 298 to 2400 K. They recommended values for the low-temperature heat capacity of the α, β, and γ phases and their entropy values at 298 K. This low-temperature information and the high-temperature enthalpy data due to Naylor [4] were used by Hillert

[1] Centro Atómico Bariloche, Consejo Nacional de Investigaciones Científicas y Técnicas, 8400 S. C. de Bariloche, Argentina.

[2] Department of Physical Metallurgy, The Royal Institute of Technology, S-10044 Stockholm, Sweden.

0195-928X/90/0900-0949$06.00/0

[5] in a new evaluation of the Gibbs energy of the various solid phases of Mn from 298 K to the melting point. He also presented expressions for liquid Mn and the gas phase. The most recent compilation of thermodynamic data of Mn, which is due to Desai [6], was published in 1987. He presented entropy values for α-, β-, and γ-Mn at 298 K, the thermal functions of the condensed phases in their stable range of temperature from 298 to 2400 K, and the properties of the gas phase.

The purpose of the present work was to evaluate the Gibbs energy functions for all condensed phases of Mn, which are necessary for performing thermodynamic calculations of binary and higher-order phase diagrams. Our treatment of the solid phases was based on recognizing the existence of a magnetic contribution to the Gibbs energy and treating it by means of a phenomenological model [7, 8] recently used to analyze the properties of Fe [9], Co [10], Ni [11], and their alloys [12–15]. In Section 2 we present the thermodynamic models for the Gibbs energy of the various Mn phases and in Section 3 we analyze the available information. In Section 4 we explain the procedure of evaluating the parameters, which we refer to in the following as optimization, and in Section 5 we discuss the results of the analysis.

2. THERMODYNAMIC MODELS

2.1. The Nonmagnetic Gibbs Energy

The present evaluation of the thermodynamic properties of Mn at atmospheric pressure, P_0, was based on resolving the Gibbs energy of the solid phases into a magnetic (ΔG_m^{mg}) and a nonmagnetic (G_m^{nmg}) contribution,

$$^{\circ}G_m(T) = G_m^{nmg}(T) + \Delta G_m^{mg}(T) \tag{1}$$

but only a nonmagnetic contribution was assumed for the liquid phase. The total Gibbs energy was referred to the enthalpy of α-Mn at $T_0 = 298.15$ K and $P_0 = 101325$ Pa, by using the expression

$$^{\circ}G_m(T) - {}^{\circ}H_m(T_0) = -{}^{\circ}S_m(T_0)T - \int_{T_0}^{T}\left[\int_{T_0}^{T} C_p^{nmg}\frac{dT}{T}\right]dT + \Delta G_m^{mg} \tag{2}$$

where C_P^{nmg} is the nonmagnetic contribution to the heat capacity. In view of the limited information available, a simple three-parameter expression was adopted to treat C_P^{nmg} below the melting point,

$$C_P^{nmg}(T) = -(c + 2dT + 2eT^{-2}) \tag{3}$$

where the coefficients c, d, and e were evaluated from experimental data or estimated. The term with T^{-2}, which may be related to the leading term of the high-temperature expansion of the vibrational heat capacity [16], was included in Eq. (3) in order to account for the C_P data on solid Mn below room temperature (cf. Section 3.4.3). The linear term in Eq. (3) may be interpreted [17] in terms of two contributions, an electronic contribution and a contribution from anharmonic effects (cf. Section 3.4.4). Equation (3) predicts a roughly linear dependence of C_P^{nmg} with temperature at high temperatures (e.g. when approaching the melting point), whereas the data on various metals suggest positive deviations from the linear behavior. The simpler description given by Eq. (3) was adopted here because of the lack of C_P data at high temperatures. Above the melting point, T_f, a method of extrapolation recently adopted by the SGTE organization [18] was used which makes the heat capacity of a solid phase approach the value of the liquid,

$$C_P^s(T) = C_P^{liq}(T) + [C_P^s(T_f) - C_P^{liq}(T_f)](T/T_f)^{-10}, \qquad T > T_f \tag{4}$$

The heat capacity of the liquid phase has been measured only at temperatures close to T_f. Therefore Eq. (3) was simplified for this phase by assuming a temperature-independent heat capacity. For the extrapolation of C_P below the melting point the procedure recommended by the SGTE [18] was again adopted. In this case the heat capacity of liquid Mn below T_f was assumed to approach C_P of the α phase according to the expression,

$$C_P^{liq} = C_P^{\alpha}(T) + [C_P^{liq}(T_f) - C_P^{\alpha}(T_f)](T/T_f)^6, \qquad T < T_f \tag{5}$$

2.2. The Magnetic Gibbs Energy

The magnetic contribution to the Gibbs energy of solid Mn was described by using a phenomenological model originally presented by Inden [7] and modified by Hillert and Jarl [8]. It is based on the expression,

$$\Delta G_m^{mg,\varepsilon} = RT \ln(\beta^{\varepsilon} + 1) f^{\varepsilon}(\tau) \tag{6}$$

where $\tau = T/T_C$, T_C is the critical temperature for magnetic ordering (i.e., the Curie temperature for ferromagnetic ordering and the Néel temperature, T_N, for antiferromagnetic ordering) of the ε phase, and β is a quantity related to the total magnetic entropy $S_m^{mg,\varepsilon}(\infty)$, i.e., the quantity,

$$S_m^{mg,\varepsilon}(\infty) = \lim_{T \to \infty} [\Delta S_m^{mg,\varepsilon}(T) - \Delta S_m^{mg,\varepsilon}(0)] \tag{7.1}$$

as follows:

$$S_m^{mg,\varepsilon}(\infty) = R \ln(\beta^{\varepsilon} + 1) \tag{7.2}$$

$f^{\varepsilon}(\tau)$ in Eq. (6) represents the polynomials obtained in the series expansion made by Hillert and Jarl [8], i.e.,

$$f^{\varepsilon}(\tau) = 1 - \frac{1}{A^{\varepsilon}}\left[\frac{79}{140}\frac{\tau^{-1}}{p^{\varepsilon}} + \left(\frac{474}{497}\right)\left(\frac{1}{p^{\varepsilon}} - 1\right)\left(\frac{\tau^3}{6} + \frac{\tau^9}{135} + \frac{\tau^{15}}{600}\right)\right] \qquad \text{for} \quad \tau < 1 \tag{8}$$

and

$$f^{\varepsilon}(\tau) = -\frac{1}{A^{\varepsilon}}\left[\frac{\tau^{-5}}{10} + \frac{\tau^{-15}}{315} + \frac{\tau^{-25}}{1500}\right] \qquad \text{for} \quad \tau > 1 \tag{9}$$

where

$$A^{\varepsilon} = \frac{518}{1125} + \frac{11692}{15975}\left[(1/p^{\varepsilon}) - 1\right] \tag{10.1}$$

and the parameter p^{ε} represents the fraction of the total magnetic enthalpy [i.e., of $\Delta H_{\mathrm{m}}^{\mathrm{mg},\varepsilon}(\infty) - \Delta H_{\mathrm{m}}^{\mathrm{mg},\varepsilon}(0)$] that is absorbed above T_{C},

$$p^{\varepsilon} = \frac{\Delta H_{\mathrm{m}}^{\mathrm{mg},\varepsilon}(\infty) - \Delta H_{\mathrm{m}}^{\mathrm{mg},\varepsilon}(T_{\mathrm{C}})}{\Delta H_{\mathrm{m}}^{\mathrm{mg},\varepsilon}(\infty) - \Delta H_{\mathrm{m}}^{\mathrm{mg},\varepsilon}(0)} \tag{10.2}$$

Although theoretical treatments suggest [19] a dependence of p^{ε} upon the structure and the magnetic moment of the ε phase, only the effect of structure is considered here, adopting the more empirical approach used by Inden [7]. He evaluated the p^{ε} parameter from experimental data on various metals and alloys and suggested the value $p = 0.4$ for the bcc(cI2) structure. It was used to treat δ-Mn(cI2). The value obtained by Inden for the fcc(cF4) structure, $p = 0.28$, was used to treat γ-Mn(cF4). Lacking information on the p parameter for α-Mn(cI58) the value $p = 0.28$ was also used, as an approximation. The final expressions of $f(\tau)$ for α-, γ-, and δ-Mn obtained by introducing these approximations in Eqs. (8) and (9) are presented in Table I, whereas β-Mn(cP20) was treated by us as if it had no magnetic transition (cf. Section 3.2.2).

2.3. The Total Gibbs Energy

The contributions to the Gibbs energy discussed in the previous sections give, when combined as indicated in Eq. (2), the following type of analytical expression for the Gibbs energy of solid and liquid Mn at 101,325 Pa, as a function of temperature:

$${}^{\circ}G_{\mathrm{m}}^{\varepsilon}(T) - {}^{\circ}H_{m}^{\alpha}(298.15) = a + bT + cT\ln T + dT^2 + eT^{-1} + jT^{(i+1)} + \Delta G_{\mathrm{m}}^{\mathrm{mg},\varepsilon} \tag{11}$$

Table I. The Mathematical Expressions Describing the Magnetic Contribution to the Gibbs Energy of α-, γ-, and δ-Mn[a]

$AG_m^{mg,\varepsilon} = RT\ln(\beta^\varepsilon + 1)\cdot f^\varepsilon(\tau)$, with $\tau = T/T_N^\varepsilon$, and T_N^ε, β, and $f^\varepsilon(\tau)$ given in the following				
Phase	Structure	T_N^ε (K)	β^ε	$f^\varepsilon(\tau)$
δ-Mn	cI2	580	0.27	$f^\varepsilon(\tau) = 1 - 0.905299383\tau^{-1} - 0.153008346\tau^3 - 0.006800370956\tau^9 - 0.00153008346\tau^{15}$, $\tau < 1$ $f^\varepsilon(\tau) = -0.0641731208\tau^{-5} - 0.00203724193\tau^{-15} - 4.27820805\ 10^{-4}\ \tau^{-25}$, $\tau > 1$
α-Mn	cI58	95	0.22	$f^\varepsilon(\tau) = 1 - 0.860338755\tau^{-1} - 0.17449124\tau^3 - 0.00775516624\tau^9 - 0.0017449124\tau^{15}$, $\tau < 1$
γ-Mn	cF4	540	0.62	$f^\varepsilon(\tau) = -0.0426902268\tau^{-1} - 0.0013552453\tau^{-15} - 2.84601512\ 10^{-4}\ \tau^{-25}$, $\tau > 1$

[a] β-Mn was treated here as if it had no magnetic transition down to 0 K. The values of T_N and β for the various phases are discussed in Sections 3.2 and 3.3, respectively.

The exponent i is equal to -10 for solid phases and equal to 6 for the liquid phase. The coefficient j is equal to zero for the solid phases below T_f and for the liquid phase above T_f. Otherwise it is obtained from Eqs. (4) and (5).

3. ANALYSIS OF THE EXPERIMENTAL INFORMATION, AND PARAMETER ESTIMATIONS

3.1. Solid/Solid and Solid/Liquid Transition Temperatures

Four allotropic forms of Mn have been reported [20], α-Mn(cI58), β-Mn(cP20), γ-Mn(cF4), and δ-Mn(cI2). The solid/solid transition temperatures selected by Hultgren et al. [3], converted to the IPTS68 temperature scale by Desai [6], were adopted in the present work. They are 980(±20) K ($\alpha \rightarrow \beta$), 1360(±10) K ($\beta \rightarrow \gamma$), and 1411(±5) K ($\gamma \rightarrow \delta$). For the melting point of δ-Mn, the value $T_f = 1519(\pm 5)$ K, selected in Ref. 6 was adopted.

3.2. Magnetic Transition Temperatures and Magnetic Moments

3.2.1. α-Mn

α-Mn was shown by Shull and Wilkinson [21] to be antiferromagnetic, with a Néel temperature of about 100 K. A close value

was reported from heat capacity measurements [22]. The value $T_N = 95(\pm 1)$ K, in agreement with the results of more recent electrical resistivity [23] and thermal expansivity measurements [24], was selected in the present work. The early neutron diffraction study by Shull and Wilkinson [21] suggested an average magnetic moment per atom (n_B) in Bohr magnetons (μ_B) of about 0.5. More recent neutron diffraction results have been resolved by assigning different magnetic moments to each one of the four different kinds of sites (I, II, III, IV) which can be distinguished in the unit cell of α-Mn [25–27]. A weighted-average moment $n_B = 0.7(\pm 0.2)$ is used by us to represent that type of information.

3.2.2. β-Mn

Neutron diffraction [25] and nuclear magnetic resonance (NMR) experiments [28] revealed that no magnetic ordering appears in β-Mn down to 1.5 K, although a weak antiferromagnetic ordering may be induced by small amounts of impurity elements [29–32]. We have therefore treated β-Mn as if it had no magnetic transition down to 0 K.

3.2.3. γ-Mn

Extrapolations from the properties of quenched fcc alloys of Mn with Cu, Ni, Pd, and Fe [33–36] have suggested that γ-Mn is antiferromagnetic and a value $n_B = 2.3(\pm 0.1)$ for the magnetic moment has been presented [34, 35]. Using the empirical correlation between atomic moment and Néel temperature for fcc alloys presented by Tauer and Weiss [37], we estimate $T_N = 540(\pm 40)$ K, which falls within the scatter band of the results of previous extrapolations in various systems [34, 36–39].

3.2.4. δ-Mn

δ-Mn is stable only between 1411 and 1519 K, the melting point. Its magnetic properties are not known. Weiss and Tauer [2] treated it as antiferromagnetic, and this assumption has not been contradicted by recent band-structure calculations [40, 41]. It was thus accepted in the present work. The order of magnitude of the n_B value for δ-Mn was estimated by comparing with the atomic moments for the Mn atoms obtained in studies of bcc Fe-Mn alloys (1.0 [42], $0.7(\pm 0.25)$ [43], 0.8 [44]), and bcc Cr-Mn alloys (0.85 [45, 46]). The average value $n_B = 0.9(\pm 0.1)$ was adopted. Using the Tauer and Weiss [37] correlation between T_N and n_B for bcc alloys, we obtained $T_N = 580(\pm 60)$ K.

3.3. Magnetic Entropy

In this section we consider the evaluation of the β parameter, which describes the total magnetic entropy [Eq. (7.2)]. The theoretical background of some of the expressions used here may be found, e.g., in recent monographs by Grimvall [47, 48]. An enlarged version of this section is given in Ref. 49.

3.3.1. General Considerations

A magnetic contribution to the entropy of α-Mn at 298 K [$S_m^{mg,\alpha}(T_0)$] was evaluated from the experimental entropy [$^\circ S_m^\alpha(T_0) = 32.2\ J \cdot mol^{-1} \cdot K^{-1}$] given by Desai [6] by subtracting a vibrational contribution ($S_m^{vib,\alpha}$) and an electronic contribution ($S_m^{el,\alpha}$),

$$S_m^{mg,\alpha} = {}^\circ S_m^\alpha - S_m^{vib,\alpha} - S_m^{el,\alpha} \tag{12}$$

The electronic contribution was approximated by applying at $T = T_0$ the expression [47],

$$S_m^{el,\alpha} = \frac{\gamma^\alpha}{1+\lambda^\alpha} T \tag{13}$$

where γ is the electronic heat capacity coefficient obtained in low-temperature experiments, and λ is an electron–phonon enhancement factor [47]. With the experimental [50] value $\gamma^\alpha = 12.8\ mJ \cdot mol^{-1} \cdot K^{-2}$ and the estimated value $\lambda^\alpha = 0.4$ [47], we obtain $S_m^{el,\alpha} = 2.7\ J \cdot mol^{-1} \cdot K^{-1}$. The leading terms in the high-temperature expansion of the vibrational entropy are

$$S_m^{vib,\alpha} = 3R\left\{\frac{4}{3} + \ln\left[\frac{T}{\theta^\alpha(0)}\right] + \cdots\right\} \tag{14}$$

Here R is the gas constant, $\theta^\alpha(0)$ is a high-temperature entropy-Debye temperature related to the logarithmic average of the phonon frequencies. This is a special case of the Debye temperatures $\theta^\alpha(n)$ which are derived from the nth moment of the phonon frequencies [48]. For instance $\theta(-3)$ is the ordinary Debye temperature obtained from the low-temperature limit of the heat capacity, and $\theta(2)$ gives the high-temperature part of the heat capacity for harmonic vibrations. Since $\theta(0)$ for paramagnetic α-Mn is not available, our evaluation of $S_m^{mg,\alpha}$ was based on the approximation [49] $\theta^I = \theta(0)$, where θ^I is a Debye temperature determined by Gazzara et al. [51] from X-ray intensity data. With the value $\theta^I = 385(\pm 10)$ K [51] we found $S_m^{mg,\alpha}(T_0) = 1.64\ J \cdot mol^{-1} \cdot K^{-1}$. Finally, relying on the fact that the Néel temperature for α-Mn is low, we approximate $S_m^{mg,\alpha}(\infty) \approx S_m^{mg,\alpha}(T_0)$, and using Eq. (7.2) we evaluate $\beta^\alpha = 0.22(\pm 0.1)$.

3.3.2. γ-Mn and δ-Mn

The quantity β for γ-Mn was treated as a free parameter in the optimization procedure (Section 4), which was controlled by the thermochemical information available (cf. Section 3.4.3). Our result is $\beta^{\gamma} = 0.62(\pm 0.3)$. The uncertainty is discusssed in Ref. 49. With the present β^{γ} value, Eq. (7.2) gives $S_m^{mg,\gamma}(\infty) = 4.0\ J \cdot mol^{-1} \cdot K^{-1}$, which is smaller than the total magnetic entropy deduced by Weiss and Tauer [2], $9.8\ J \cdot mol^{-1} \cdot K^{-1}$.

The available experimental information on δ-Mn does not allow an evaluation of β^{δ} by means of the optimization procedure described in Section 4. This parameter was estimated from the n_B^{δ} value, by assuming that the ratio $\beta^{\delta}/n_B^{\delta}$ is roughly the same as for the other modifications. Adopting $\beta^{\delta}/n_B^{\delta} = 0.3(\pm 0.1)$ and $n_B^{\delta} = 0.9(\pm 0.1)$ (from Section 3.2.4), we obtained $\beta^{\delta} = 0.27(\pm 0.1)$. This values gives $S_m^{mg,\delta}(\infty) = 2.0(\pm 0.7)\ J \cdot mol^{-1} \cdot K^{-1}$, which is smaller than Weiss and Tauer's [2] result, $S_m^{mg,\delta}(\infty) = 5.8\ J \cdot mol^{-1} \cdot K^{-1}$.

3.4. Enthalpy and Heat Capacity of the Solid Phases

3.4.1. α-Mn

In addition to the ${}^{\circ}S_m^{\alpha}(298.15)$ value (cf. Section 3.3.1), six low-temperature heat capacity values between 200 and 270 K were selected from Desai [6], eight heat-capacity measurements between 373 and 1073 K from Armstrong and Grayson-Smith [52], and seven enthalpy values between 400 and 1000 K from Naylor [4].

3.4.2. β-Mn

In addition to ${}^{\circ}S_m^{\beta}(298.15)$ [6] and the α/β equilibrium temperature we selected six low-temperature heat capacity values between 200 and 270 K from Desai [6], a single heat capacity value at 1073 K from Armstrong and Grayson-Smith [52], and four enthalpy values from Naylor [4] between 1000 and 1400 K.

3.4.3. γ-Mn: Room-Temperature Properties

Although γ-Mn is stable over a limited temperature range, between 1360 and 1411 K, some information on its properties at and below room temperature is available. The entropy at 298.15 K evaluated by Desai [6], ${}^{\circ}S_m^{\gamma}(298.15) \approx 33.2\ J \cdot mol^{-1} \cdot K^{-1}$, was used to evaluate $\theta^{\gamma}(0)$. The separation of the electronic contribution was based on the experimental [53]

value $\gamma^{\gamma} = 9.2\ 10^{-3}\ \mathrm{J \cdot mol^{-1} \cdot K^{-2}}$ and the estimated value $\lambda^{\gamma} = 0.4$ [47]. We obtained $\theta^{\gamma}(0) = 331$ K. Low-temperature experiments suggest (Table VI) $\theta^{\gamma}(-3) = 370$ K. The ratio, $\theta^{\gamma}(0)/\theta^{\gamma}(-3) = 331/370 \approx 0.89$, is comparable with the average for elements of the 3d, 4d, and 5d series given in Ref. 54, which is $\theta(0)/\theta(-3) \approx 0.8(\pm 0.1)$. Information on $C_{\mathrm{P}}^{\gamma}(298.15)$ is also available [6] and was included in the optimization. The heat capacity at lower temperatures is determined by the parameter e^{γ} of the present description of $C_{\mathrm{P}}^{\mathrm{nmg},\gamma}$, Eq. (3). It was defined from a comparison with the coefficient of the T^{-2} term in the high-temperature expansion of the vibrational (harmonic) heat capacity, $C^{\mathrm{vib}}(T)$, which is [48]

$$C^{\mathrm{vib}} \approx 3R\left[1 - \frac{1}{20}\left(\frac{\theta(2)}{T}\right)^2 + \cdots\right] \tag{15.1}$$

The comparison gives

$$e^{\gamma} \approx \frac{3R}{40}\theta^2(2) \tag{15.2}$$

Introducing in Eq. (15.2) the approximation $\theta^{\gamma}(2) \approx \theta^{\gamma}(0) = 331$ K we obtained $e^{\gamma} = 6.96\ 10^4\ \mathrm{J \cdot mol^{-1} \cdot K}$, which leads to C_{P} values in agreement with experiments [6] down to 200 K.

3.4.4. γ-Mn: High-Temperature Heat Capacity

In addition to the β/γ equilibrium temperature we included in the optimization three enthalpy values at 1374, 1400, and 1410 K measured by Naylor [4]. The temperature range covered by these enthalpy measurements is not large enough for an accurate evaluation of C_{P}^{γ} at high temperatures. A probable behavior for C_{P}^{γ} in that range was defined by using the procedure recently applied by Fernández Guillermet and Grimvall [17]. They analyzed the slope of the $C_{\mathrm{P}}^{\mathrm{nmg}}$ vs T curve for technetium at high temperatures in terms of the expression

$$\left[\frac{\partial C_{\mathrm{P}}}{\partial T}\right]_{\mathrm{P}} = \frac{\gamma}{1+\lambda} - \frac{3R}{\theta^{\mathrm{S}}}\left[\frac{\partial \theta^{\mathrm{S}}}{\partial T}\right]_{\mathrm{P}} \tag{16}$$

Here $\theta^{\mathrm{S}}(T)$ is a temperature-dependent entropy Debye temperature [55] which is evaluated from the vibrational part of the experimental entropy, $S_{\mathrm{m}}^{\mathrm{vib}}(T)$ (cf. Section 3.3.1), by solving the implicit equation,

$$S_{\mathrm{m}}^{\mathrm{vib}}(T) = S_{\mathrm{D}}(T/\theta^{\mathrm{S}}) \tag{17}$$

where S_{D} is the Debye model expression for the entropy. Due to anharmonicity, the vibrational frequencies change with temperature. Hence $\theta^{\mathrm{S}}(T)$

in Eq. (17) is temperature dependent. In line with the results of a recent analysis of $\theta^S(T)$ [56] for various transition metals, we assumed that the relative decrease in $\theta^S(T)$ with T for γ-Mn at high temperatures [i.e., the second term in Eq. (16)], which is not known, is the same as of α-Mn, and get from Eq. (16) an approximated relation between the slopes of the C_P^{nmg} vs T curves. When applied in the high-temperature limit, where Eq. (3) gives $(\partial C_P^{nmg}/\partial T)_P = -2d$, we get the following estimate of the d parameter for γ-Mn

$$d^\gamma = d^\alpha + \frac{1}{2}\left[\frac{\gamma^\alpha}{1+\lambda^\alpha} - \frac{\gamma^\gamma}{1+\lambda^\gamma}\right] \tag{18}$$

Inserting in Eq. (18) the values $d^\alpha \approx -7.35\ 10^{-3}\ \mathrm{J \cdot mol^{-1} \cdot K^{-2}}$, evaluated from the experimental data on α-Mn (cf. Section 3.4.1), $\gamma_\alpha = 12.8\ 10^{-3}\ \mathrm{J \cdot mol^{-1} \cdot K^{-2}}$ [50], $\gamma^\gamma = 9.2\ 10^{-3}\ \mathrm{J \cdot mol^{-1} \cdot K^{-2}}$ [53], and the approximation $\lambda^\alpha = \lambda^\gamma = 0.4$ [47], we get $d^\gamma = -6.0\ 10^{-3}\ \mathrm{J \cdot mol^{-1} \cdot K^{-2}}$.

3.4.5. δ-Mn: Debye Temperature and Estimated Parameters

In addition to the γ/δ equilibrium temperature we included in the optimization two enthalpy values, at 1410 and 1450 K, reported by Naylor [4]. The parameters c^δ and e^δ in Eq. (3), which describe the behavior at lower temperatures, were estimated. The quantity e^δ was estimated using Eq. (15.2) with a value for $\theta^\delta(0)$ obtained from the expression

$$S_m^{vib,\delta} - S_m^{vib,\gamma} = \Delta S_m^{vib,\gamma\to\delta} \approx 3R\left\{\ln\left[\frac{\theta^\gamma(0)}{\theta^\delta(0)}\right]\right\} \tag{19}$$

which is derived from Eq. (14). Inserting the value $\Delta S_m^{vib,\gamma\to\delta} = 0.2(\pm 0.1)R$ proposed in Ref. 57 and $\theta^\gamma(0) = 331$ K obtained in Section 3.4.3, in Eq. (19), we get $\theta^\delta(0) = 310(\pm 10)$ K. Then, Eq. (15.2) yields $e^\delta = 6.0(\pm 0.4)\ 10^4\ \mathrm{J \cdot mol^{-1} \cdot K}$. The parameter c^δ was given a value such that the heat capacity of δ-Mn at room temperature is comparable with the values for the other solid phases. With the value $c^\delta = -23.7\ \mathrm{J \cdot mol^{-1} \cdot K^{-1}}$, adopted in the present work, we have $C_P^\delta(298.15) \approx 26.8\ \mathrm{J \cdot mol^{-1} \cdot K^{-1}}$, which is in line with the average for the other phases, $27(\pm 0.8)\ \mathrm{J \cdot mol^{-1} \cdot K^{-1}}$.

3.5. Properties of the Liquid Phase

3.5.1. Enthalpy and Entropy of Fusion

Values of the enthalpy of fusion ($\Delta_f H$) of Mn have been presented by Braun et al. [58] and by Sato and Kleppa [59]. Braun et al. [58]

used high-temperature adiabatic calorimetry and reported $\Delta_f H_m = 14.1(\pm 0.2)\,\mathrm{kJ \cdot mol^{-1}}$, which corresponds to an entropy of fusion $\Delta_f S \approx 9.3(\pm 0.1)\,\mathrm{J \cdot mol^{-1} \cdot K^{-1}}$. Sato and Kleppa [59] used an indirect procedure, based on determining the enthalpy difference between γ-Mn and liquid Mn($^\circ H^{liq}_{Mn} - {}^\circ H^{\gamma}_{Mn}$) at 1386 K by measuring the partial molar enthalpy of solution of γ-Mn($H^{liq}_{Mn} - {}^\circ H^{\gamma}_{Mn}$) in Mn–Ni alloys of various Mn contents ($0.505 \leqslant x_{Mn} \leqslant 0.757$) and extrapolating to pure Mn. Here H^{liq}_{Mn} denotes the partial molar enthalpy of Mn in the Mn–Ni solution. In Fig. 1 we plot the $H^{liq}_{Mn} - {}^\circ H^{\gamma}_{Mn}$ values determined by Sato and Kleppa [59] vs $(1 - x_{Mn})^2$ together with two lines. The solid represents the one adopted by them for extrapolating to $x_{Mn} = 1$. It corresponds to a rapidly varying interaction parameter in the Mn–Ni solutions (cf. our discussion in Ref. 49) and gives $^\circ H^{liq}_{Mn} - {}^\circ H^{\gamma}_{Mn} \approx 12.8\,\mathrm{kJ \cdot mol^{-1}}$. Using this value and other information on the properties of γ-, δ-, and liquid Mn taken from Hultgren et al. [3], Sato and Kleppa [59] estimated the enthalpy of fusion of δ-Mn, $\Delta_f H_m \approx 11.0(\pm 0.8)\,\mathrm{kJ \cdot mol^{-1}}$ [i.e., $\Delta_f S_m \approx 7.24(\pm 0.5)\,\mathrm{J \cdot mol^{-1} \cdot K^{-1}}$], which is (roughly) $3\,\mathrm{kJ \cdot mol^{-1}}$ lower than the result by Braun et al. [58]. The dashed line in Fig. 1, which represents a least-squares fit to their points, and is consistent with a regular-solution behavior of the liquid phase [49], would give $^\circ H^{liq}_{Mn} - {}^\circ H^{\gamma}_{Mn} \approx 14\,\mathrm{kJ \cdot mol^{-1}}$, which is higher than the value by Sato and Kleppa [59] by $14 - 12.86 \approx 1.2\,\mathrm{kJ \cdot mol^{-1}}$. We conclude that without using additional information on the properties of the Mn–Ni system, one could very well obtain from the data in Fig. 1 a higher value

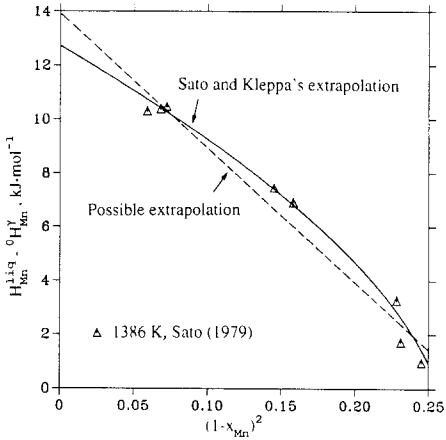

Fig. 1. The partial enthalpy of solution of γ-Mn in liquid Mn–Ni solutions, at 1386 K, according to experimental data of Sato and Kleppa [59] and two possible extrapolations to pure manganese.

Table II. The Enthalpy and Entropy of Fusion and the Heat Capacity of Liquid Mn According to Various Sources

Source of information	$\Delta_f H_m$ ($kJ \cdot mol^{-1}$)	$\Delta_f S_m$ ($J \cdot mol^{-1} \cdot K^{-1}$)	C_P ($J \cdot mol^{-1} \cdot K^{-1}$)	Comments
Hultgren et al. [3]	12.10	7.95	46.0	Estimated values
Braun et al. [58]	14.10	9.28	47.3 to 47.9	Experimental values
Sato and Kleppa [59]	11.0 ($\pm$0.8)	7.24 ($\pm$0.5)	—	Based on an extrapolated value for ${}^{\circ}H^{liq}_{Mn} - {}^{\circ}H^{\gamma}_{Mn}$ at 1386 K
Hillert [5]	12.1	7.95	46.0	Selected values from Ref. 3
Desai [6]	11.0 ($\pm$0.8)	7.24 ($\pm$0.5)	46.0	Selected values: $\Delta_f H_m$ from Ref. 59, C_P from Ref. 3
Present work	12.9 ($\pm$1.5)	8.5 ($\pm$1)	48.0 ($\pm$1)	cf. Section 3.5

of the enthalpy of melting of δ-Mn, say, $\Delta_f H_m \approx 12\ kJ \cdot mol^{-1}$, i.e., $\Delta_f S_m \approx 7.9\ J \cdot mol^{-1} \cdot K^{-1}$. Lacking further information which could help to solve the remaining discrepancy of $2\ kJ \cdot mol^{-1}$ with Braun et al. [58], we choose for $\Delta_f H_m$ a value in between, based on adopting for Mn an entropy of fusion $\Delta_f S_m \approx 8.5(\pm 1)\ J \cdot mol^{-1} \cdot K^{-1}$, which fits smoothly a plot of $\Delta_f S_m$ vs the number of d electrons [49]. The $\Delta_f S_m$ value proposed here gives $\Delta_f H_m \approx 12.9(\pm 1.5)\ kJ \cdot mol^{-1}$.

3.5.2. Heat Capacity

Some information on the heat capacity for liquid Mn at and above the melting point was presented by Braun et al. [58]. In agreement with their results we adopted $C_P = 48(\pm 1)\ J \cdot mol^{-1} \cdot K^{-1}$ (Table II). This value also fits smoothly a plot of C_P vs the number of d electrons [49].

4. PARAMETER OPTIMIZATION

The evaluation of the various model parameters was made by using PARROT, a computer program for the optimization of thermodynamic parameters developed by Jansson [60]. The program works by minimizing an error sum where each experimental data value has been given an appropriate weight. The weights were selected by personal judgment and they were changed by trial and error during the work until reasonable agreement was obtained for most of the information. A summary of parameters describing the thermodynamic properties of Mn above 298 K is

Table III. Summary of Optimum Parameters for Manganese at $P_0 = 101325$ Pa[a]

α-Mn

$298.15 < T < 1519$ K

$$^{\circ}G_m^{\alpha}(T) - {}^{\circ}H_m^{\alpha}(T_0) = -8115.28 + 130.059T - 23.4582T \ln T - 7.34768\ 10^{-3}\ T^2 + 69827.1T^{-1} + \Delta G_m^{mg,\alpha}$$

$1519 < T < 2500$ K

$$^{\circ}G_m^{\alpha}(T) - {}^{\circ}H_m^{\alpha}(T_0) = -28733.41 + 312.2648T - 48T \ln T + 1.656847\ 10^{30}\ T^{-9}$$

β-Mn

$298.15 < T < 1519$ K

$$^{\circ}G_m^{\beta}(T) - {}^{\circ}H_m^{\alpha}(T_0) = -5800.4 + 135.995T - 24.8785T \ln T - 5.83359\ 10^{-3}\ T^2 + 70269.1T^{-1}$$

$1519 < T < 2500$ K

$$^{\circ}G_m^{\beta}(T) - {}^{\circ}H_m^{\alpha}(T_0) = -28290.76 + 311.2933T - 48T \ln T + 3.967567\ 10^{30}\ T^{-9}$$

γ-Mn

$298.15 < T < 1519$ K

$$^{\circ}G_m^{\gamma}(T) - {}^{\circ}H_m^{\alpha}(T_0) = -3439.3 + 131.884T - 24.5177T \ln T - 6\ 10^{-3}\ T^2 + 69600T^{-1} + \Delta G_m^{mg,\gamma}$$

$1519 < T < 2500$ K

$$^{\circ}G_m^{\gamma}(T) - {}^{\circ}H_m^{\alpha}(T_0) = -26070.1 + 309.6664T - 48T \ln T + 3.8619645\ 10^{30}\ T^{-9}$$

δ-Mn

$298.15 < T < 1519$ K

$$^{\circ}G_m^{\delta}(T) - {}^{\circ}H_m^{\alpha}(T_0) = -3235.3 + 127.85T - 23.7T \ln T - 7.44271\ 10^{-3}\ T^2 + 60000T^{-1} + \Delta G_m^{mg,\delta}$$

$1519 < T < 2500$ K

$$^{\circ}G_m^{\delta}(T) - {}^{\circ}H_m^{\alpha}(T_0) = -23188.83 + 307.7043T - 48T \ln T + 1.265152\ 10^{30}\ T^{-9}$$

Liquid Mn

$298.15 < T < 1519$ K

$$^{\circ}G_m^{liq}(T) - {}^{\circ}H_m^{\alpha}(T_0) = 9744.63 + 117.4382T - 23.4582T \ln T - 7.34768\ 10^{-3}\ T^2 + 69827.1T^{-1} - 4.4192927\ 10^{-21}\ T^7$$

$1519 < T < 2500$ K

$$^{\circ}G_m^{liq}(T) - {}^{\circ}H_m^{\alpha}(T_0) = -9993.9 + 299.036T - 48T \ln T$$

[a] All values in SI units. Temperature values according to IPTS 68 ($R = 8.31451$ J · mol^{-1} · K^{-1}). $T_0 = 298.15$ K. $H_m^{\alpha}(T_0) - H_m^{\alpha}(0) = 5188(\pm 10)$ J · mol^{-1} is taken from Desai [6]. $\Delta G_m^{mg,\varepsilon}$ (with $\varepsilon = \alpha, \gamma, \delta$) is given in Table I.

given in Table III. The magnetic contribution to the Gibbs energy of α-, γ-, and δ-Mn is described using the expressions given in Table I. All thermodynamic calculations reported in the following were performed using POLY, a computer program for equilibrium calculations developed by Jansson [60]. Values of various thermodynamic properties of Mn between 298.15 and 2500 K are presented in Table IV.

Table IV. Calculated Thermodynamic Properties of Manganese at 101,325 Pa, $T_0 = 298.15$ K

T (K)	C_P ($J \cdot mol^{-1} \cdot K^{-1}$)	$^\circ H(T) - ^\circ H(T_0)$ ($kJ \cdot mol^{-1}$)	$^\circ S - ^\circ S(0)$ ($J \cdot mol^{-1} \cdot K^{-1}$)	$^\circ G - ^\circ H^\alpha(T_0)$ ($kJ \cdot mol^{-1}$)
298.15(α)	26.273	0.0000	32.220	−9.6065
300	26.319	0.0486	32.383	−9.6663
400	28.464	2.7926	40.262	−13.312
500	30.247	5.7300	46.809	−17.674
600	31.887	8.8375	52.470	−22.644
700	33.460	12.105	57.505	−28.148
800	34.996	15.528	62.073	−34.130
900	36.511	19.103	66.283	−40.550
980(α)	37.714	22.072	69.442	−45.981
980(β)	36.166	24.326	71.742	−45.981
1000	36.405	25.052	72.475	−47.423
1100	37.596	28.752	76.001	−54.849
1200	38.781	32.571	79.323	−62.616
1300	39.962	36.508	82.474	−70.707
1360(β)	40.669	38.927	84.293	−75.711
1360(γ)	40.796	41.093	85.885	−75.711
1400	41.275	42.734	87.075	−79.170
1411(γ)	41.407	43.189	87.398	−80.130
1411(δ)	44.672	45.097	88.751	−80.130
1500	45.996	49.132	91.523	−88.153
1519(δ)	46.279	50.009	92.104	−89.897
1519(liq)	48.000	62.918	100.60	−89.897
1600	48.000	66.806	103.09	−98.148
1700	48.000	71.606	106.00	−108.60
1800	48.000	76.406	108.75	−119.34
1900	48.000	81.206	111.34	−130.34
2000	48.000	86.006	113.80	−141.60
2100	48.000	90.806	116.14	−153.10
2200	48.000	95.606	118.38	−164.83
2300	48.000	100.40	120.51	−176.78
2400	48.000	105.20	122.55	−188.93
2500(liq)	48.000	110.00	124.51	−201.28

Table V. The Enthalpies of the Allotropic Transitions in Manganese According to Various Sources

Source of information	Enthalpy of the transition ($J \cdot mol^{-1}$)		
	$\alpha \rightarrow \beta$	$\beta \rightarrow \gamma$	$\gamma \rightarrow \delta$
Naylor [4]	2238 (±?)	2280 (±?)	1799 (±?)
Weiss and Tauer [2]	2272 (±200)	2393 (±200)	1975 (±200)
Hultgren et al. [3]	2226 (±200)	2121 (±335)	1879 (±335)
Hillert [5]	2266	2311	1895
Desai [6]	2225 (±200)	2120 (±330)	1879 (±335)
Present work	2254	2166	1908

5. DISCUSSION

5.1. High-Temperature Enthalpy and Enthalpies of Allotropic Transitions

The enthalpy of α-, β-, γ-, and δ-Mn, calculated using the description given in Table III, reproduces very well the experimental data of Naylor [4] (Fig. 2). In Fig. 3 we compare the calculated enthalpy of solid Mn with the early measurements by Wüst et al. [61], which were not used in the optimization. His data for α-Mn are well reproduced by the calculation, but the calculated enthalpy for β-Mn falls above the data points from the

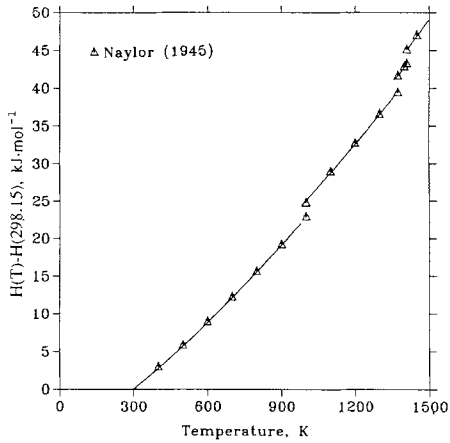

Fig. 2. The enthalpy of α-, β-, γ-, and δ-Mn calculated using the present description (Table III), compared with experimental data reported by Naylor [4].

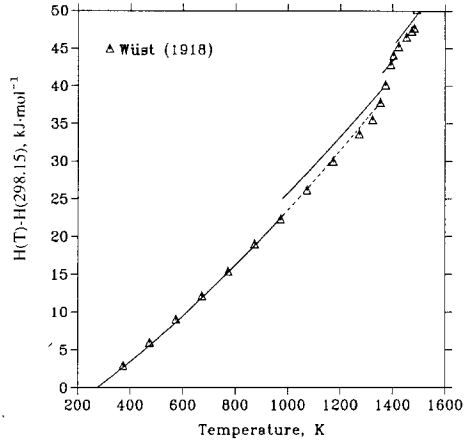

Fig. 3. The enthalpy of α-, β-, γ-, and δ-Mn calculated using the present description (Table III), compared with experimental data reported by Wüst et al. [61]. These data were not used for parameter evaluation. The dashed line represents the calculated enthalpy of metastable α-Mn.

stable range of temperature for this phase. Consideration of the extrapolated enthalpy of α-Mn (dashed line) suggests that metastable states may have been involved in Wüst and co-workers' [61] experiments. The calculated enthalpy of γ-Mn falls within the experimental scatter band of his points, but for δ-Mn, the calculation, based on a fit to Naylor's [4] data, gives larger values. The evaluated enthalpies of the allotropic transitions in Mn are compared in Table V with values according to various sources.

Table VI. Properties of the Mn Phases at 298.15 K and at Low Temperatures, According to Various Sources

	Room temperature			Low temperature	
Phase	C_P ($J \cdot mol^{-1} \cdot K^{-1}$)	$^\circ S$ ($J \cdot mol^{-1} \cdot K^{-1}$)	θ (K)	γ ($mJ \cdot mol^{-1} \cdot K^{-2}$)	θ (K)
α-Mn	26.27 (a)[a]	32.22 (a)	385 (±10) (c)	12.8 (e)	409 (e)
β-Mn	26.78 (a)	34.90 (a)	—	—	—
γ-Mn	27.96 (a)	33.15 (a)	331 (d)	9.2 (f)	370 (g)
δ-Mn	27.29 (b)	34.17 (b)	310 (±10) (b)	—	—

[a] (a) According to Ref. 6; (b) present estimate, see text; (c) θ^I, experimental, from Ref. 51; (d) present evaluation, see text; (e) experimental, from Ref. 50; (f) experimental, from Ref. 53; (g) experimental, from Ref. 64.

5.2. High-Temperature Heat Capacity

5.2.1. α-Mn

In Fig. 4 we compare the calculated heat capacity of Mn between 200 and 1600 K with experimental data due to Armstrong and Grayson-Smith [52]. All experimental points fall below the calculated line, and the discrepancy is particularly large between 600 and 900 K. When analyzing low-temperature data also reported by Armstrong and Grayson-Smith [62], Hultgren et al. [3] concluded that their samples could have been contaminated with β-Mn. The fact that the extrapolated C_P curve for the β phase (dashed line in Fig. 4) roughly accounts for the data points between 600 and 900 K suggests that the conclusion by Hultgren et al. [3] may apply at high temperatures as well.

5.2.2. β-Mn

According to the present evaluation, there is a decrease in C_P associated with the $\alpha \rightarrow \beta$ allotropic transition. This feature is shared with the descriptions presented by Weiss and Tauer [2] and Hillert [5]. On the other hand, according to Hultgren et al. [3] and Desai [6], $C_P^{\beta} > C_P^{\alpha}$ at the transition temperature. Besides, the slope of the C_P^{β} vs T curve $((\partial C_P^{\beta}/\partial T)_P)$, in their descriptions is much smaller than for the α phase.

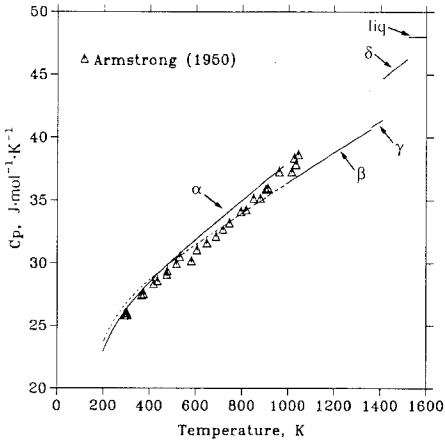

Fig. 4. The heat capacity of α-, β-, γ-, δ-, and liquid Mn calculated using the present description (Table III), compared with experimental data reported by Armstrong and Grayson-Smith [52]. The dashed line represents the heat capacity of metastable β-Mn.

The present description of β-Mn gives more similar slopes $(\partial C_P^{\beta}/\partial T)_P \approx 0.80(\partial C_P^{\alpha}/\partial T)_P$.

5.2.3. γ-Mn

Since the stable range for the γ phase is very narrow, previous analysis of Mn have been based on making some assumptions on the temperature dependence of its C_P. They are reviewed elsewhere [49]. Here we used a different procedure, based on Eq. (16); cf. Section 3.4.4. It gives for the slope of the C_P^{γ} vs T curve at high temperatures $(\partial C_P^{\gamma}/\partial T)_P \approx 0.82(\partial C_P^{\alpha}/\partial T)_P$. This result is very close to that obtained for β-Mn (5.2.2) and implies that the difference in C_P associated with the $\beta \rightarrow \gamma$ transition is very small (Fig. 4). It leads to smaller C_P values than proposed in previous works.

5.2.4. δ-Mn

The present description of the properties of δ-Mn was constructed by combining Naylor's [4] enthalpy data with estimated values of the low-temperature properties and the total magnetic entropy and optimizing the parameter which controls the slope of the heat capacity vs T curve at high temperatures. The optimized description gives, when approaching T_f, $(\partial C_P^{\delta}/\partial T)_P \approx (\partial C_P^{\alpha}/\partial T)_P$. This is demonstrated in Fig. 5. In the stable range of temperature, our description gives C_P^{δ} values which are comparable to those presented by Hultgren et al. [3] and by Desai [6].

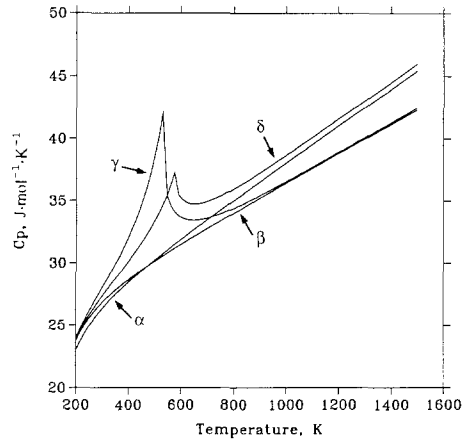

Fig. 5. The heat capacity of α-, β-, γ-, and δ-Mn calculated using the present description (Table III), illustrating the effect of the magnetic transition on C_P of γ-Mn ($T_N^{\gamma} = 540$ K) and δ-Mn ($T_N^{\delta} = 580$ K).

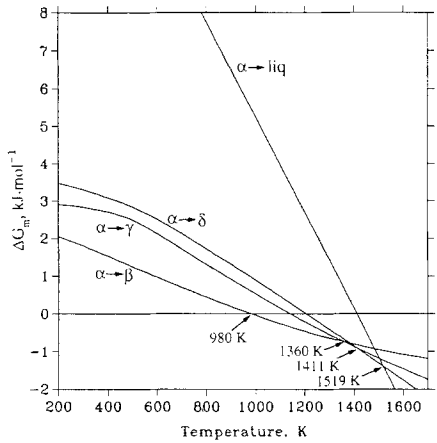

Fig. 6. Gibbs energy differences between the various Mn phases and the α phase. $\alpha \rightarrow \varepsilon$ means ${}^{\circ}G_{\mathrm{m}}^{\varepsilon} - {}^{\circ}G_{\mathrm{m}}^{\alpha}$. The temperatures for the various stable phase transitions and the metastable melting points of α-, β-, and γ-Mn are given in Sections 3.1 and 5.3, respectively.

5.3. Lattice Stabilities and Metastable Melting Points

In Fig. 6 we present the evaluated Gibbs energy of the various condensed phases of Mn, referred to the Gibbs energy of the α phase. These Gibbs energy differences are often called lattice stabilities [63]. These curves are further considered in Ref. 49. In Fig. 6 we present a curve representing the difference ${}^{\circ}G_{\mathrm{m}}^{\mathrm{liq}} - {}^{\circ}G_{\mathrm{m}}^{\alpha}$ according to the present work. The intersections of this curve with the other lines define the melting points of the various phases. We obtain the following metastable melting points: 1411 K (α-Mn), 1484 K (β-Mn), and 1503 K (γ-Mn).

ACKNOWLEDGMENTS

It is a privilege to acknowledge valuable comments on this paper by Professor Mats Hillert and many illuminating discussions with Professor Göran Grimvall. This research was partially supported by the Swedish Board for Technical Development (STU).

REFERENCES

1. K. J. Tauer and R. J. Weiss, *J. Phys. Chem. Solids* **2**:237 (1957).
2. R. J. Weiss and K. J. Tauer, *J. Phys. Chem. Solids* **4**:135 (1958).
3. R. Hultgren, P. D. Desai, D. T. Hawkins, M. Gleiser, K. K. Kelley, and D. D. Wagman, *Selected Values for the Thermodynamic Properties of the Elements* (American Society for Metals, Metals Park, Ohio, 1973), pp. 301–308.
4. B. F. Naylor, *J. Chem. Phys.* **13**:329 (1945).
5. M. Hillert, *Trita-Mac-0305* (Revised) (Royal Institute of Technology, Stockholm, Sweden, Feb. 1986).
6. P. D. Desai, *J. Phys. Chem. Ref. Data* **16**:91 (1987).
7. G. Inden, *Project Meeting Calphad V. Ch. 111, 4* (Düsseldorf, Max Planck Institut Eisenforsch., 1976), pp. 1–13.
8. M. Hillert and M. Jarl, *Calphad* **2**:227 (1978).
9. A. Fernández Guillermet and P. Gustafson, *High Temp. High Press.* **16**:591 (1985).
10. A. Fernández Guillermet, *Int. J. Thermophys.* **8**:481 (1987).
11. A. Dinsdale, Unpublished (National Physical Laboratory, Teddington, Middlesex, U.K., 1985).
12. A. Fernández Guillermet, *High Temp. High Press.* **19**:477 (1987).
13. A. Fernández Guillermet, *Z. Metallkunde* **78**:639 (1987).
14. Zhong Shu Xing, D. D. Gohil, A. T. Dinsdale, and T. Chart, National Physical Laboratory DMA (A) 103, London (1985).
15. A. Fernández Guillermet, *Calphad* **13**:1 (1989).
16. H. Thirring, *Phys. Z.* **14**:867 (1913); O. Stern, *Ann. Phys. Leipzig* **51**:237 (1916).
17. A. Fernández Guillermet and G. Grimvall, *J. Less-Common Metals* **147**:195 (1989).
18. J. O. Andersson, A. Fernández Guillermet, P. Gustafson, M. Hillert, B. Jansson, B. Jönsson, B. Sundman, and J. Ågren, *Calphad* **11**:95 (1987).
19. A. Paskin, *J. Phys. Chem. Solids* **2**:232 (1957).
20. J. Donohue, *The Structures of the Elements* (R. E. Krieger, Malabar, Fla., 1982), pp. 191–200.
21. C. G. Shull and M. K. Wilkinson, *Rev. Modern Phys.* **25**:100 (1953).
22. P. Franzosini and C. G. Losa, *Z. Naturforsch.* **19A**:1348 (1964).
23. N. Mori and T. Mitsui, *Phys. Lett.* **39A**:413 (1972).
24. N. S. Petrenko, V. P. Popov, and V. A. Finkel, *Phys. Lett.* **47A**:471 (1974).
25. J. S. Kasper and B. W. Roberts, *Phys. Rev.* **15**:537 (1956).
26. J. A. Oberteuffer, J. A. Marcus, L. H. Schwartz, and G. P. Felcher, *Phys. Rev.* **B2**:670 (1970).
27. T. Yamada, N. Kunitomi, Y. Nakai, D. E. Cox, and G. Shirane, *J. Phys. Soc. Jap.* **28**:615 (1970).
28. Y. Masuda, K. Asayama, S. Kobayashi, and J. Itoh, *J. Phys. Soc. Jap.* **19**:460 (1964).
29. T. Kohara and K. Asayama, *J. Phys. Soc. Jap.* **37**:401 (1974).
30. S. Akimoto, T. Kohara, and K. Asayama, *Sol. State Comm.* **16**:1227 (1975).
31. M. Katayama and K. Asayama, *J. Phys. Soc. Jap.* **44**:425 (1978).
32. T. Shinkoda, K. I. Kumagai, and K. Asayama, *J. Phys. Soc. Jap.* **46**:1754 (1979).
33. D. Meneghetti and S. S. Sidhu, *Phys. Rev.* **105**:130 (1957).
34. G. E. Bacon, I. W. Dunmur, J. H. Smith, and R. Street, *Proc. Roy. Soc.* **A241**:223 (1957).
35. T. J. Hicks, A. R. Pepper, and J. H. Smith, *J. Phys. C* **1**:1683 (1968).
36. Y. Ishikawa, H. Sekine, and K. Yamada, *J. Phys. Soc. Jap.* **37**:874 (1974).
37. K. J. Tauer and R. J. Weiss, *Phys. Rev.* **100**:1223 (1955).
38. H. Masumoto, S. Sawaya, and M. Kikuchi, *J. Jap. Inst. Metals* **35**:723 (1971).
39. M. P. Ravdel and O. I. Yevdokimova, *Izv. Akad. Nauk. SSSR Metally* **5**:204 (1973).

40. J. Kübler, *J. Mag. Magn. Mater.* **20**:107 (1980).
41. G. Fuster, N. E. Brener, J. Callaway, J. L. Fry, Y. Z. Zhao, and D. A. Papaconstantopoulos, *Phys. Rev. B* **38**:423 (1988).
42. S. G. Kang, H. Onodera, H. Yamamoto, and H. Watanabe, *J. Phys. Soc. Jap.* **36**:975 (1974).
43. Y. Nakai and N. Kunitomi, *J. Phys. Soc. Jap.* **39**:1257 (1975).
44. H. Yamauchi, H. Watanabe, Y. Suzuki, and H. Saito, *J. Phys. Soc. Jap.* **36**:971 (1974).
45. J. S. Kasper and R. M. Waterstrat, *Phys. Rev.* **109**:1551 (1958).
46. Y. Hamaguchi and N. Kunitomi, *J. Phys. Soc. Jap.* **19**:1849 (1964).
47. G. Grimvall, *The Electron-Phonon Interaction in Metals* (North-Holland, Amsterdam, 1981).
48. G. Grimvall, *Thermophysical Properties of Materials* (North-Holland, Amsterdam, 1986).
49. A. Fernández Guillermet and Weiming Huang, *Trita-Mac-0396* (Royal Institute of Technology, Stockholm, Sweden, Apr. 1989).
50. G. L. Guthrie, S. A. Friedberg, and J. E. Goldman, *Phys. Rev.* **139**:1200 (1965).
51. C. P. Gazzara, R. M. Middleton, and R. J. Weiss, *Phys. Lett.* **10**:257 (1964).
52. L. D. Armstrong and H. Grayson-Smith, *Can. J. Res.* **28A**:51 (1950).
53. J. C. Ho and N. E. Phillips, *Phys. Lett.* **10**:34 (1964).
54. A. Fernández Guillermet and G. Grimvall, *Phys. Rev. B* **40**:1521 (1989).
55. G. Grimvall and J. Rosén, *Int. J. Thermophys.* **4**:139 (1982); J. Rosén and G. Grimvall, *Phys. Rev. B* **27**:7199 (1983).
56. M. Thiessen, *Int. J. Thermophys.* **9**:159 (1988). See also G. Grimvall, M. Thiessen, and A. Fernández Guillermet, *Phys. Rev. B* **36**:7816 (1987).
57. A. Fernández Guillermet and M. Hillert, *Calphad* **12**:337 (1988).
58. M. Braun, R. Kohlhaas, and O. Vollmer, *Z. Angew. Phys.* **25**:365 (1968).
59. S. Sato and O. J. Kleppa, *J. Chem. Thermodyn.* **11**:521 (1979).
60. B. Jansson, *Computer Operated Methods for Equilibrium Calculations and Evaluation of Thermodynamic Model Parameters*, Ph.D. thesis (Dept. Phys. Met., Royal Institute of Technology, Stockholm, Sweden, 1984).
61. F. Wüst, A. Meuthen, and R. Durrer, *Forschungsarbeiten Auf dem Gebiete des Ingenieurwesens, No. 204* (Springer, Berlin, 1918).
62. L. D. Armstrong and H. Grayson-Smith, *Can. J. Res.* **27A**:9 (1949).
63. L. Kaufman and H. Bernstein, *Computer Calculation of Phase Diagrams* (Academic Press, New York, 1970); cf. also Ref. 57.
64. N. E. Phillips, *Crit. Rev. Solid State Sci.* **2**:467 (1971).